c-Jun N-terminal kinase 2 deficiency protects against hypercholesterolemia-induced endothelial dysfunction and oxidative stress

Osto, E ; Matter, C M ; Kouroedov, A ; Malinski, T ; Bachschmid, M ; Camici, G G ; Kilic, U ; Stallmach, T ; Boren, J ; Iliceto, S ; Lüscher, T F ; Cosentino, F

Abstract: BACKGROUND: Hypercholesterolemia-induced endothelial dysfunction due to excessive production of reactive oxygen species is a major trigger of atherogenesis. The c-Jun-N-terminal kinases (JNKs) are activated by oxidative stress and play a key role in atherogenesis and inflammation. We investigated whether JNK2 deletion protects from hypercholesterolemia-induced endothelial dysfunction and oxidative stress. METHODS AND RESULTS: Male JNK2 knockout (JNK2(-/-)) and wild-type (WT) mice (8 weeks old) were fed either a high-cholesterol diet (HCD; 1.25% total cholesterol) or a normal diet for 14 weeks. Aortic lysates of WT mice fed a HCD showed an increase in JNK phosphorylation compared with WT mice fed a normal diet ($P<0.05$). Endothelium-dependent relaxations to acetylcholine were impaired in WT HCD mice ($P<0.05$ versus WT normal diet). In contrast, JNK2(-/-) HCD mice did not exhibit endothelial dysfunction (96+/-5% maximal relaxation in response to acetylcholine; $P<0.05$ versus WT HCD). Endothelium-independent relaxations were identical in all groups. A hypercholesterolemia-induced decrease in nitric oxide (NO) release of endothelial cells was found in WT but not in JNK2(-/-) mice. In parallel, endothelial NO synthase expression was upregulated only in JNK2(-/-) HCD animals, whereas the expression of antioxidant defense systems such as extracellular superoxide dismutase and manganese superoxide dismutase was decreased in WT but not in JNK2(-/-) HCD mice. In contrast to JNK2(-/-) mice, WT HCD displayed an increase in O(2)(-) and ONOO(-) concentrations as well as nitrotyrosine staining and peroxidation. CONCLUSIONS: JNK2 plays a critical role as a mediator of hypercholesterolemia-induced endothelial dysfunction and oxidative stress. Thus, JNK2 may provide a novel target for prevention of vascular disease and atherosclerosis.

DOI: https://doi.org/10.1161/CIRCULATIONAHA.108.765032

JNK2 Deficiency Protects Against Hypercholesterolemia-Induced Endothelial Dysfunction and Oxidative Stress

[1,2]Elena Osto MD, [1,2]Christian M. Matter MD, [1,2]Alexey Kouroedov MD, PhD, [3]Tadeusz Malinski PhD, [4]Markus Bachschmid PhD, [1,2] Giovanni Camici PhD, [1,2] Ulkan Kilic PhD, [5]Thomas Stallmach MD, [6]Jan Boren PhD, [7]Sabino Iliceto MD, [1,2]Thomas F. Luscher MD,[1,2,8]Francesco Cosentino MD, PhD

[1]Cardiology and Cardiovascular Research, Institute of Physiology and University Hospital; [2]Zurich Center for Integrative Human Physiology (ZIHP), University of Zurich, Switzerland;[3] Department of Biochemistry, Ohio University, Athens, Ohio; [4]Department of Medicine, Boston University School of Medicine, Boston, Massachusetts; [5]Department of Pathology, University Hospital, Zurich, Switzerland; [6]Wallenberg Laboratory Sahlgrenska Academy, Goteborg, Sweden, [7] Cardiology, University of Padua, [8]Cardiology, 2nd Faculty of Medicine, University "Sapienza", Rome, Italy,

Running title: Role of *JNK2* in endothelial dysfunction

Address for Correspondence: Francesco Cosentino, M.D., Ph.D.
Cardiology & Cardiovascular Research
Institute of Physiology
University of Zurich-Irchel
Winterthurerstrasse, 190
CH-8057 Zurich, Switzerland
Tel: 41-44-635 5097
Fax: 41-44-635 6827
Email: f_cosentino@hotmail.com

Abstract

Background: Hypercholesterolemia-induced endothelial dysfunction due to excessive production of reactive oxygen species (ROS) is a major trigger of atherogenesis. The c-Jun-N-terminal kinases (JNK) are activated by oxidative stress and play a key role in atherogenesis and inflammation. We investigated whether *JNK2* deletion protects from hypercholesterolemia-induced endothelial dysfunction and oxidative stress.

Methods and results: Male *JNK2* knockout (*JNK2*$^{-/-}$) and wild-type (WT) mice (8 weeks old) were fed either a high cholesterol (HCD; 1.25% total cholesterol) or a normal diet (ND) for 14 weeks. Aortic lysates of WT mice fed a HCD showed an increase in JNK phosphorylation compared with WT mice fed a ND ($p<0.05$). Endothelium-dependent relaxations to acetylcholine were impaired in WT HCD mice ($p<0.05$ vs. WT ND). In contrast, *JNK2*$^{-/-}$ HCD mice did not exhibit endothelial dysfunction (96±5% max relaxation to Ach, $p<0.05$ vs. WT HCD). Endothelium-independent relaxations were identical in all groups. Hypercholesterolemia-induced decrease in NO release of endothelial cells was found in WT but not in *JNK2*$^{-/-}$ mice. In parallel, eNOS expression was upregulated only in *JNK2*$^{-/-}$ HCD animals, whereas the expression of antioxidant defense systems such as EC-SOD and Mn-SOD was decreased in WT, but not in JNK2$^{-/-}$ HCD mice. In contrast to *JNK2*$^{-/-}$ mice, WT HCD displayed an increase in O_2^- and $ONOO^-$ concentrations as well as of nitrotyrosine staining and peroxidation.

Conclusions: JNK2 plays a critical role as a mediator of hypercholesterolemia-induced endothelial dysfunction and oxidative stress. Thus, JNK2 may provide a novel target for prevention of vascular disease and atherosclerosis.

Key words: JNK, endothelium, atherosclerosis, reactive oxygen species, nitric oxide, cholesterol.

Introduction

Atherosclerosis is a systemic immunoinflammatory disease developing in response to endothelial injury (1). Indeed, the endothelium is a key determinant of vascular integrity. Hypercholesterolemia, a well-known risk factor for cardiovascular disease, leads to accumulation and oxidation of LDL-cholesterol within the intima of the vessel wall triggering endothelial dysfunction and pro-inflammatory milieu as crucial steps in the early phase of the atherosclerotic process (2). Oxidative stress, resulting from an imbalance between reactive oxygen species (ROS) and antioxidant defense system, is a crucial mediator of hypercholesterolemia-induced endothelial dysfunction (3,4). Indeed, ROS interact and inactivate nitric oxide (NO) and lead to protein nitration and lipid peroxidation.

The c-Jun N-terminal kinases (JNKs), also known as stress-activated protein kinases (SAPK), are serin/threonin protein kinases belonging to the mitogen-activated protein kinase (MAPK) superfamily (5). JNKs play a fundamental role in stress responses, cell survival and apoptosis. The JNK pathway is activated by stress factors such as UV and radiation, reperfusion injury, ceramides, and inflammatory cytokines (6). The dimerization of JNK leads to activation of other kinases, their nuclear translocation and subsequent modulation of the activity of different transcription factors such as c-Jun, ATF-2, Elk-1, p-53 and c-myc (7).

Three distinct *JNK* genes have been described, *JNK1*, *JNK2*, and *JNK3*, encoding for different isoforms. *JNK3* expression is restricted to brain, heart and testis, while *JNK1* and *JNK2* proteins are ubiquitously expressed (8). Both *JNK1*- and *JNK2*-deficient mice are viable indicating that neither *JNK1* nor *JNK2* play an essential role in development and normal cellular functions; however, genetic disruption of both *JNK1* and *JNK2* is lethal (9).

Studies using gene targeting as wells as JNK inhibitors demonstrated the involvement of *JNK1* and *JNK2* genes in several pathological conditions including cancer, immune and neurological diseases as well as metabolic disorders and inflammatory conditions such as arthritis and atherosclerosis (10).

JNKs are expressed in vascular smooth muscle cells (VSMC) and endothelial cells (EC) and activated by a wide range of stimuli such as oxidative stress, mechanical stretch, hypertension (11-13), hyperglycemia, apoptosis (14) or inflammation (10). A recent study suggested a role of JNK in endothelial dysfunction: short-term exposure of coronary arterioles to TNFα-induced endothelial dysfunction through activation of *JNK* signal transduction pathway and generation of superoxide anion (15). We recently reported a critical role of *JNK2* in atherogenesis showing that *JNK2* is required for foam cell formation within the atherosclerotic plaque by activating the scavenger receptor A (SR-A) (16).

The role of *JNK2* in the early stage of atherosclerosis related to endothelial dysfunction as it occurs under hypercholesterolemic conditions remains unknown. Thus, we compared *JNK2*-deficient to wild-type mice exposed to a high cholesterol or a normal diet. We found that endogenous *JNK2* is critically involved in hypercholesterolemia-induced endothelial dysfunction and oxidative stress.

Materials and Methods

Animals and diets

JNK2$^{-/-}$ and WT mice (both in a C57BL/6J background) were obtained from Jackson Laboratory (Bar Harbor, ME) and kept on a regular diet. Mice were housed in temperature-controlled cages (20-22◦C), fed ad libitum and maintained on a12:12-hour light–dark cycle. At the age of 8 weeks, mice were fed a normal (ND) or a high cholesterol diet (HCD, D12108 containing 1.25% cholesterol, Research Diets, New Brunswick, NJ) for 14 weeks, respectively. All animal experiments were approved by the local Institutional Animal Care Committee

Plasma lipid measurements

At the time of tissue harvesting, 0.5 to 1 ml of blood was drawn from the right ventricle with heparinized syringes, immediately centrifuged at 4°C, and the plasma stored at -80°C. Total cholesterol, triglycerides, and free fatty acids were analyzed using the reagents TR13421, TR22421 (both Thermo Electron Clinical Chemistry & Automation Systems) and 994-75409 (Wako Chemicals GmbH, Germany), as recommended by the manufacturer. The lipid distribution in plasma lipoprotein fractions was assessed by fast-performance liquid chromatography gel filtration with a Superose 6 HR 10/30 column (Pharmacia, Sweden).

Tissue harvesting

Mice were euthanized by intraperitoneal administration of 50 mg/kg sodium pentobarbital. The entire aorta from the heart to the iliac bifurcation was excised and placed immediately in cold modified Krebs-Ringer bicarbonate solution (pH 7.4, 37°C, 95% O2; 5% CO2) of the following composition (mmol/L): NaCl (118.6), KCl (4.7), CaCl2 (2.5), KH2PO4 (1.2), MgSO4 (1.2), NaHCO3 (25.1), glucose (11.1), and calcium EDTA (0.026). The aorta was

cleaned from adhering connective tissue under a dissection microscope, and either snap-frozen in liquid nitrogen and stored at -80°C or used immediately for organ chamber experiments.

Organ chamber experiments

For endothelial function experiments, aortae were cut into rings (2 to 3 mm long). Each ring was connected to an isometric force transducer (Multi-Myograph 610M, Danish Myo Technology, Denmark), suspended in an organ chamber filled with 5 mL Krebs-Ringer bicarbonate solution (37°C, pH 7.4), and bubbled with 95% O_2, 5% CO_2. Isometric tension was recorded continuously. After a 30 minute equilibration period, rings were gradually stretched to the optimal point of their length–tension curve as determined by the contraction in response to potassium chloride (100 mmol). Concentration–response curves were obtained in a cumulative fashion. Several rings cut from the same artery were studied in parallel. Responses to acetylcholine (Ach, 10^{-9} to 10^{-6} mol/L, Sigma Aldrich) in the presence or absence of polyethylene glycol-superoxide dismutase (PEG-SOD, 150 U/ml, Sigma Aldrich) were recorded during submaximal contraction to norepinephrine (NE, 10^{-6} mol/L). The NO donor sodium nitroprusside (SNP, 10^{-10} to 10^{-5} mol/L, Sigma Aldrich) was added to test endothelium-independent relaxation. Relaxations were expressed as a percentage of the precontracted tension.

Measurements of NO, O_2^- and $ONOO^-$

Concurrent measurements of NO, O_2^- and $ONOO^-$ were carried out with three electrochemical nanosensors combined into one working unit with a total diameter of 2.0 - 2.5 µm. Their design was based on previously developed and well-characterized chemically modified carbon-fiber technology (4,17,18). Amperometry was performed with a computer-based Gamry VFP600 multichannel potentiostat. A current at the peak potential

characteristic for NO (0.65 V) oxidation and $ONOO^-$ (-0.40 V) or O_2^- (-0.23 V) reduction was directly proportional to the local concentrations of these compounds in the immediate vicinity of the sensor. Linear calibration curves (current vs. concentration) were constructed for each sensor from 10 nmol/L to 2 μmol/L before and after measurements with aliquots of NO, O_2^- and $ONOO^-$ standard solutions, respectively. At a constant distance of the sensors from the surface of the endothelial cell, the reproducibility of measurements is high (5-12%). The consumption of redox species by nanosensors depends on the area of the electrode (< 0.12 μm^2) and the duration time of electrolysis (~5-10 s). For the amperometric measurements used, it varied between 0.04-0.1% of the NO, $O_2^-$and $ONOO^-$ peak concentration. This value is negligible compared with the experimental error. The position of nanosensors (*x,y, z* coordinates) versus the endothelial cell was established with the help of a computer controlled micromanipulator. In order to establish a constant distance from cells, the module of sensors was lowered until it reached the surface of the cell membrane. After that, the sensors were slowly raised 4 $\pm$ 1 μm (*z* coordinates) from the surface of cells. The sensors were then moved horizontally (*x, y* coordinates) and positioned above a surface of randomly chosen single endothelial cells in an aortic ring. Acetylcholine (Ach), were then injected with a nanoinjector that was also positioned by a computer controlled-micromanipulator.

Western blotting

Frozen samples of aortae were pulverized and dissolved in lysis buffer (120 mmol/L sodium chloride, 50 mmol/L Tris, 20 mmol/L sodium fluoride, 1 mmol/L benzamidine, 1 mmol/L DTT, 1 mmol/L EDTA, 6 mmol/L EGTA, 15 mmol/L sodium pyrophosphate, 0.8 μg/mL leupeptin, 30 mmol/L *p*-nitrophenyl phosphate, 0.1 mmol/L PMSF, and 1% NP-40) for immunoblotting. Cell debris were removed by centrifugation (12 000 *g*) for 10 minutes at 4°C. The samples (20 μg) were treated with 5x Laemmli's SDS-PAGE sample buffer

(0.35 mol/L Tris-Cl, pH 6.8, 15% SDS, 56.5% glycerol, 0.0075% bromophenol blue), followed by heating at 99°C for 5 minutes, and then subjected to 10% SDS-PAGE gel for electrophoresis. The proteins were then transferred onto Immobilon-P filter papers (Millipore AG, Bedford, MA) with a semidry transfer unit (Hoefer Scientific, San Francisco, CA). The membranes were then blocked by use of 5% skim milk in TBS-Tween buffer (0.1% Tween 20; pH 7.5) for 1 hour at room temperature and incubated with anti total JNK and p-JNK; (1:1000, Santa Cruz Biotechnology, Inc), anti-NOS3 rabbit polyclonal antibody (1:1000 dilution; Santa Cruz Biotechnology, Inc), anti-phospho (Ser1177) –eNOS rabbit polyclonal antibody (1:250, Cell Signaling), anti-MnSOD rabbit polyclonal antibody (1:2000 dilution, Upstate USA, Inc), anti-Cu/ZnSOD rabbit polyclonal antibody (1:2000; Upstate Biotechnology) and anti-ECSOD (1:1000; Upstate Biotechnology) for 1 hour at room temperature. Membranes were then incubated with the secondary antibody (horseradish peroxidase–conjugated anti-mouse/rabbit immunoglobulin antibody; Amersham Pharmacia Biotech) at a dilution of 1:2000. Prestained markers (Bio-Rad Laboratories) were used for molecular mass determinations. The immunoreactive bands were detected by an enhanced chemiluminescence kit (Amersham Biosciences). Anti-α-tubulin mouse monoclonal antibody (1:2000) or anti-β–actin (1:1000, Sigma Aldrich) was employed as a loading control. Western blots were quantified densitometrically (NIH Image 1.6, Bethesda, MD).

Immunohistochemistry and superoxide detection

Freshly isolated aortic segments were immediately embedded in O.C.T. medium and snap frozen in pentane/liquid nitrogen. Cryosections of 6 μm thickness were mounted on SuperFrost glass slides and incubated at 37°C for 30 min with 1 μM dihydroethidium for superoxide detection. In order to stain for protein-bound nitrotyrosine or MnSOD, sections were fixed in 4% PBS-buffered formalin for 5 min, blocked with 10% BSA in PBS and

incubated with polyclonal anti-nitrotyrosine antibody (1:50; Upstate) and anti-MnSOD antibody (1:250; StressGen) at 4°C overnight, respectively. For visualization, the secondary antibody (Alexa568 anti-rabbit IgG; 1:300; Molecular Probes) was incubated for 1h at room temperature. Slides were then rinsed, embedded in glycerin-PBS and examined under a fluorescent microscope (DM-IRB; Leica) connected to a digital imaging system (Spot-RT; Diagnostic Instruments/Visitron Systems, Germany). Pictures were obtained using identical camera and microscope settings. Dihydroethidium-stained specimens were background-corrected for autofluorescence of elastic fibers and the basal lamina using ImageJ/ NIH (rsb.info.nih.gov/ij/).

Thiobarbituric acid reactive substances (TBARS) assay

In vitro assessment of aortic levels of lipid peroxidation was performed using TBARS Assay Kit (OXItek, ZeptoMetrix, New York), according to the manufacturer's instructions. Briefly, snap frozen tissue was crushed in a pre-chilled mortar and pestle and resuspended at a concentration of 50 mg/ml in PBS. 100 μl of homogenate were then added to SDS solution and thoroughly mixed. Following TBA/buffer reagent addition, samples were incubated at 95°C for 60 minutes and centrifuged at 3000 rpm at room temperature for 15 minutes. Absorbance was read at 532 nm.

Statistical analysis

Results are expressed as mean±SEM and n indicates number of experiments. Statistical analysis was performed with Student's *t* test for simple comparisons between 2 values. For multiple comparisons results were analyzed by ANOVA followed by Bonferroni post-hoc correction. A value of $p<0.05$ was considered statistically significant.

The authors had full access to and take full responsibility for the integrity of the data. All authors have read and agree to the manuscript as written.

Results

Lipid profiles

We determined plasma cholesterol, triglycerides and free fatty acids in *JNK2*$^{-/-}$ and WT mice fed either a HCD or a ND (Table 1). Both *JNK2*$^{-/-}$ and WT mice developed significant hypercholesterolemia after 14 weeks of HCD. Interestingly, *JNK2*$^{-/-}$ mice had slight but significantly increased levels of total plasma cholesterol compared with WT mice either on ND or HCD (Table 1). No difference in plasma triglycerides or free fatty acids was observed between the groups (Table 1).

Hypercholesterolemia activates aortic JNK

To determine the effect of hypercholesterolemia on JNK activation, we compared Western blot analyses of aortic lysates from normo- and hypercholesterolemic WT mice using a phosphospecific JNK antibody. Aortae from WT mice on HCD showed increased JNK phosporylation compared with vessels from WT on ND (Figure 1).

JNK2 deletion protects from hypercholesterolemia-induced endothelial dysfunction

Isometric tension studies demonstrated no difference in vascular contractions to norepinephrine (NE) between aortae obtained from WT or *JNK2*$^{-/-}$ mice fed either a HCD or ND (data not shown). Endothelium-dependent relaxations to acetylcholine were impaired in WT mice on HCD compared with WT mice on ND. Interestingly, endothelium-dependent relaxations remained normal in *JNK2*$^{-/-}$ HCD mice, suggesting a preserved $^{\bullet}$NO bioavailability favored by the lack of *JNK2* (Figure 2A). Concurrent with this notion, addition of the free radical scavenger PEG-SOD (150U/mL) significantly improved endothelium-dependent relaxations in HCD WT mice (Figure 2B). Endothelium-

independent relaxations to sodium nitroprusside were similar in all groups (data not shown).

Preserved endothelial NO release in hypercholesterolemic *JNK2*$^{-/-}$ mice

For assessing NO bioavailability at the level of endothelial cells, we determined NO in single endothelial cells using nanonsensors. After stimulation with acetylcholine (10^{-7} mol/L), maximal NO levels were 242$\pm$10 nmol/L in WT mice on ND, and decreased about 50% in WT mice on HCD (Figure 3A). In contrast, similar levels of NO release were found in *JNK2*$^{-/-}$ mice on ND or HCD (Figure 3A).

Decreased oxidative stress in hypercholesterolemic *JNK2*$^{-/-}$ mice

To determine the effect of hypercholesterolemia on oxidative stress in endothelial cells, we measured superoxide anion (O_2^-) and peroxynitrite ($ONOO^-$) production in single aortic endothelial cells. A significant increase in O_2^- concentration was observed in WT mice exposed to HCD compared with WT mice on a ND, whereas no significant hypercholesterolemia-induced changes were observed in *JNK2*$^{-/-}$ mice (Figure 3B and C). In agreement with preserved NO bioavailability and O_2^- findings, $ONOO^-$ concentrations were increased only in WT, but not in *JNK2*$^{-/-}$ mice fed a HCD (Figure 4A). Since $ONOO^-$ leads to increased 3-nitrotyrosine-containing proteins, we performed in situ immunohistochemistry with a polyclonal antibody against 3-nitrotyrosine in aortic cross-sections. *JNK2*$^{-/-}$ HCD mice showed a markedly reduced immunoreactivity both in the endothelium and in the media compared with diet-matched WT mice (Figure 4B). This favourable redox profile was confirmed measuring aortic TBARS levels. Following HCD exposure, *JNK2*$^{-/-}$ mice did not exhibit an increase in lipid peroxidation compared with WT mice (Figure 4C).

Free radical scavenger expression and activity

Protein expression of three pivotal free radical scavengers was assessed to determine whether an upregulation of antioxidant defense mechanisms might explain the preserved NO bioavailability in hypercholesterolemic *JNK2*$^{-/-}$ mice. Cu/Zn-SOD was similar in all experimental groups (data not shown), whereas aortic expression of manganese (Mn) and extracellular (EC) SOD was significantly decreased in WT mice fed a HCD compared with WT mice on a ND (Figure 5A and B). By contrast, levels of Mn-SOD and EC-SOD in *JNK2*$^{-/-}$ HCD were similar to WT ND mice (Figures 5A and B). Unexpectedly, *JNK2*$^{-/-}$ ND exhibited a reduced expression of both SOD isoforms compared with diet-matched WT mice (Figures 5A and B). Accordingly, immunofluorescent stainings for MnSOD showed similar results in aortic cross-sections (Figure 5C).

Increased eNOS expression in *JNK2*$^{-/-}$ mice

In order to get more insight into the mechanisms of preserved NO bioavailability in *JNK2*$^{-/-}$ mice with hypercholesterolemia, we quantified eNOS expression in aortic lysates. eNOS expression was not affected by HCD in WT mice, whereas *JNK2*$^{-/-}$ HCD mice showed a significant increased expression of eNOS (Figure 6A). Furthermore, to determine whether NO production was also regulated by eNOS activity, we performed additional blotting of phosphorylated Ser1177-eNOS in pooled samples. pS1177-eNOS protein levels were similar in aortic lysates from *JNK2*$^{-/-}$ on either diet and WT mice on ND. In contrast, we found reduced eNOS phosphorylation in WT mice on HCD (Figure 6B).

Discussion

This study for the first time demonstrates that genetic deletion of *JNK2* protects against hypercholesterolemia-induced and ROS-mediated endothelial dysfunction. The following findings support our conclusion: 1) Chronic exposure of WT mice to a high cholesterol diet induces aortic JNK phosphorylation. 2) In contrast to WT mice, long-term exposure of *JNK2*$^{-/-}$ to HCD did not impair endothelium-dependent relaxation to acetylcholine. 3) Lower $ONOO^-$ levels in hypercholesterolemic *JNK2*$^{-/-}$ mice were associated with decreased protein nitration and lipid peroxidation. Accordingly, 4) expression of the antioxidant enzymes Mn-SOD and EC-SOD was increased in *JNK2*$^{-/-}$ mice. In contrast, we observed a downregulation of these enzymes after 14 weeks of HCD in WT mice.

Genetic deletion of JNK2 did not affect severity of hypercholesterolemia, although *JNK2*$^{-/-}$ mice had slightly but significantly increased levels of total cholesterol compared with WT mice either fed with normal or high cholesterol diet. Thus, we could rule out that differences observed among the two groups were caused by different experimental conditions. In contrast to our findings, a recent study showed similar total plasma cholesterol levels in *JNK2*$^{-/-}$ and WT controls (19).

Preserved bioavailability of NO is a key marker of vascular integrity. *In vivo*, activity of the L-arginine-NO pathway is determined by a balance between synthesis and breakdown of NO for its reaction with O_2^-. This balance is impaired in hypercholesterolemia and atherosclerosis (20,21). Endothelial dysfunction, reflected by impaired endothelium-dependent relaxation, occurs in experimental models of hypercholesterolemia as was confirmed in wild-type mice of this study (22,23). Similarly, many clinical studies reported abnormal endothelium-dependent vasodilation in hypercholesterolemic patients (24). Hypercholesterolemia induces a series of molecular events that increase the production of ROS and inactivate NO to form $ONOO^-$ (25). In this study, acetylcholine-induced relaxation

did not differ between *JNK2*$^{-/-}$ and WT mice in control conditions of normocholesterolemia following normal diet. However, upon chronic hypercholesterolemia induced by 14 weeks of HCD, WT mice but not *JNK2*$^{-/-}$ mice developed endothelial dysfunction.

The finding that addition of the free radical scavenger PEG-SOD restored endothelium-dependent relaxation in wild-type mice on a high cholesterol diet suggests an important role of reactive oxygen species in this context. Hypercholesterolemia-induced oxidative stress has been attributed to activation of oxidases in the vasculature and in infiltrating leukocytes (22). Moreover, hypercholesterolemia has been shown to impair antioxidant defense mechanisms against $ONOO^-$ formation (25).

To investigate whether preserved endothelial function in hypercholesterolemic *JNK2*$^{-/-}$ mice was associated with increased bioavailability of NO, we assessed NO release from single endothelial cells after stimulation with acetylcholine. In hypercholesterolemic control mice, NO levels decreased by about 50%, whereas they remained unchanged in *JNK2*$^{-/-}$ mice. Because O_2^- is the main inactivator of NO, we tested whether decreased endothelial production of O_2^- contributes to increased $^{\bullet}NO$ bioavailability in *JNK2*$^{-/-}$ mice. We found enhanced O_2^- production in hypercholesterolemic wild-type mice compared with mice on a normal diet, whereas no significant diet-induced changes were detected in *JNK2*$^{-/-}$ mice. Dihydroethidium stainings of aortic segments confirmed these findings.

In aortae exposed to chronic hypercholesterolemia, the reaction of NO and O_2^- leads to enhanced $ONOO^-$ formation, and in turn, increased nitrotyrosine residues which are typical end products of the reaction of $ONOO^-$ with biological compounds (26). Tyrosine nitration is responsible for inactivation of several enzymes (27). Our group has shown that nitration of MnSOD and prostacyclin synthase occur in aged and diabetic mice, respectively (28,29). In agreement with the notion that *JNK2* deficiency induces preserved NO bioavailability, but reduced O_2^- production, we found that $ONOO^-$ concentrations were increased in WT, but not in *JNK2*$^{-/-}$ mice fed a HCD. In parallel, nitrotyrosine

immunoreactivity was detected in both endothelium and smooth muscle cells of hypercholesterolemic mice, as previously shown by our group (30). However, aortae from hypercholesterolemic wild-type mice exhibited enhanced immunostaining compared with diet-matched *JNK2*$^{-/-}$ mice. $ONOO^-$ contributes to atherogenesis by promoting lipid peroxidation (31). In contrast to hypercholesterolemic wild-type mice, *JNK2*$^{-/-}$ mice were protected against lipid peroxidation as determined by TBARS in aortic lysates.

To investigate whether antioxidant defense mechanisms contribute to the preserved endothelial function in hypercholesterolemic *JNK2*$^{-/-}$ mice, we assessed protein expression of three pivotal O_2^- scavengers. Aortic expression of Mn-SOD and EC-SOD was decreased in hypercholesterolemic wild-type mice as compared to normocholesterolemic controls. By contrast, both Mn-SOD and EC-SOD were induced after 14 weeks of hypercholesterolemia in *JNK2*$^{-/-}$ mice. Furthermore, in situ immunohistochemistry showed that changes in MnSOD expression occur throughout the aortic vascular wall. These findings suggest that the ability of the SOD scavenging system to respond to oxidative stress remains intact in *JNK2*$^{-/-}$ mice. Unexpectedly, normocholesterolemic *JNK2*$^{-/-}$ mice exhibited a reduced expression of Mn-SOD and EC-SOD compared with diet-matched WT mice. However, these changes did not translate into differences in endothelium-dependent, NO-mediated responses as shown by organ chamber experiments and in situ measurements of NO release. At low concentrations, O_2^- diffusion is slow and O_2^- is scavenged by highly diffusible NO. Therefore, at low O_2^- in *JNK2*$^{-/-}$ mice on ND, SOD may be less competitive for O_2^- than NO. This process may change under high O_2^- and low NO levels as found in the context of hypercholesterolemia where the role of SOD becomes more substantial. Accordingly, the reduced expression of Mn-SOD and EC-SOD in *JNK2*$^{-/-}$ mice on ND did not translate into changes of NO, O_2^- and $ONOO^-$ production. In order to get more insight into the mechanisms of preserved NO bioavailability in hypercholesterolemic *JNK2*$^{-/-}$ mice, we assessed eNOS expression in aortic lysates.

Western blot analysis revealed higher eNOS expression in hypercholesterolemic *JNK2*$^{-/-}$ compared with wild-type mice. Conflicting data have been reported related to the regulation of eNOS during hypercholesterolemia. There is evidence of reduced transcription and enhanced breakdown of eNOS transcripts upon increasing concentrations of oxidized LDL. Long-term stimulation with oxidized LDL may also lead to a decrease in the amount of NOS protein through induction of cytokines (32). Experimental atherosclerosis is associated with an increased eNOS expression and NO production, whereas decreased eNOS expression and NO release is found in advanced human atherosclerosis (33). To determine whether NO production was also regulated by eNOS activity, we determined eNOS phosphorylation. Interestingly, the observed upregulation of eNOS protein in *JNK2*$^{-/-}$ on HCD did not translate into increased eNOS phosphorylation, justifying unchanged NO concentrations and endothelium-dependent relaxations in *JNK2*$^{-/-}$ mice. On the other hand, decreased eNOS phosphorylation in WT HCD mice matched reduced NO levels found in this group

As deletion of *JNK2* in hypercholesterolemic mice was associated with upregulation of SOD, it is likely that this antioxidant defense system contributes to protect against hypercholesterolemia-mediated oxidative stress in *JNK2*$^{-/-}$ mice. Thus, our findings suggest that *JNK2* is involved in the pathways regulating vascular endothelial ROS production and antioxidant defense systems under hypercholesterolemic conditions. Our results are in accordance with previous studies that associate JNK activation with increased levels of oxidative stress and ROS-mediated cell death (34). In particular, JNK is known to play a major role in cardiovascular disease and is activated upon mechanical stress, hypertension (11-13) and ischemia/reperfusion (35). JNK has also been reported to be activated in advanced atherosclerotic plaques in rabbits as well as in humans (34) and to activate matrix proteases involved in disease progression of abdominal aortic aneurysm in mice and humans (36). Along this line, *JNK2* is necessary for scavenger receptor A or

CD36-mediated foam cell formation in atherogenesis (16,37,38). *JNK2* has also been demonstrated to be involved in insulitis of type I diabetes mellitus (39). Pharmacologic JNK inhibition is a promising strategy given its beneficial effects in mouse models of atherogenesis (16), abdominal aneurysm (37), and cerebral ischemia (40). JNK inhibition may even be more rewarding considering its the critical role in obesity and insulin resistance (41). Thus, JNK inhibition could represent a attractive therapeutic target to prevent progression of atherosclerosis and metabolic disease. Our findings suggest that JNK may also be a promising target for preventing atherosclerosis at its early stage of endothelial dysfunction.

Funding Sources

This work was supported in part by Swiss National Research Foundation Grants 310000108463 (F.C.), 3100-068118 (T.F.L.) and 31-114094/1 (C.M.M.), and the Swiss Heart Foundation (F.C., C.M.M.) as well as a US Public Health Grant 0418061 (T.M.). The University Research Priority Program „Integrative Human Physiology“ at the University of Zurich (F.C., T.F.L., C.M.M.) and European Vascular Genomic Network (T.F.L.) also supported this study.

Acknowledgements

We would like to thank Alexander Akhmedov, PhD for genotyping *JNK2*$^{-/-}$ mice and Elisabeth Muessig for MnSOD immunostaining.

References

1. Hansson GK. Inflammation, atherosclerosis and coronary artery disease. NEJM. 2005;352: 1685-95.
2. Libby P, Ridker PM. Inflammation and atherothrombosis. From population biology and bench research to clinical practice. J Am Coll Cardiol 2006;48:A33-46.
3. Vergnani L, Hatrik S, Ricci F, Passaro A, Manzoli N, Zuliani G, Brovkovych V, Fellin R, Malinski T. Effect of native and oxidized low-density lipoprotein on endothelial nitric oxide and superoxide production - Key role of L-arginine availability. Circulation, 2000; 101:1261-1266.
4. Erdei N, Toth A, Pasztor ET, Papp Z, Edes I, Koller A, Bagi Z. High-fat diet-induced reduction in nitric oxide-dependent arteriolar dilation in rats: role of xanthine oxidase-derived superoxide anion. Am J Physiol Heart Circ Physiol 2006;291:H2107-15.
5. Ichjio H. From receptors to stress-activated MAP kinases. Oncogene. 1999;18:6087-93.
6. Kyriakis JM, Avruch J. Mammalian mitogen-activated protein kinase signal transduction pathways activated by stress and inflammation. Physiol Rev. 2001;81:807-69.
7. Jaeschke A, Karasarides M, Ventura JJ, Ehrhardt A, Zhang C, Flavell RA, Shokat KM, Davis RJ. JNK2 is a positive regulator of the cJun transcription factor. Mol Cell. 2006;23:899-911.
8. Davis RJ. Signal transduction by the JNK group of MAP kinases. Cell 2000;103:239-252.

9. Kuan CY, Yang DD, Samanta Roy DR, Davis RJ, Rakic P, Flavell RA. The Jnk1 and Jnk2 protein kinases are required for regional specific apoptosis during early brain devlopment. Neuron 1999;22:667-676.
10. Bogoyevitch M.A .The isoform-specific functions of the c-Jun N-terminal Kinases (JNKs): differences revealed by gene targeting. BioEssays 2006;28:923–934.
11. Xu Q, Liu Y, Gorospe M, Udelsman R, Holbrook NJ. Acute hypertension activates mitogen-activated protein kinases in arterial wall.J Clin Invest. 1996;97:508-14.
12. Touyz RM, Yao G. Up-regulation of vascular and renal mitogen-activated protein kinases in hypertensive rats is normalized by inhibitors of the Na+/Mg2+ exchanger. Clin Sci. 2003 ;105:235-42.
13. Touyz RM, Yao G, Viel E, Amiri F,.Schiffrin EL. Angiotensin II and endothelin-1 regulate MAP kinases through different redox-dependent mechanisms in human vascular smooth muscle cells.J Hypertens 2004;22:1141–1149.
14. Ho FM, Lin WW, Chen BC, Chao CM, Yang C, Lin LY, Lai CC, Liu SH, Liau CS. High glucose-induced apoptosis in human vascular endothelial cell is mediated trough NF-kB and c-Jun NH2-terminal kinase pathway and prevented by PI3K/Akt/eNOS pathway. Cell Sign 2006;18:391-399.
15. Zhang C, Hein T, Wang W, Ren y, Shipley RD, Kuo L. Activation of JNK and xanthine oxidase by TNF-α impairs nitric oxide-mediated dilation of coronary arterioles. J Moll Cell Cardiol 2006;40:247-57.
16. Ricci R, Sumara G, Sumara I, Rozemberg I, Kurrer M, Akhmedov A, Hersberger M, Eriksson U, Eberli F, Becher B, Boren J, Chen M, Cybulsky MI, Moore KJ, Freeman MV, Wagner EF, Matter CM, Luscher TF. Requirement of JNK2 for scavenger receptor A-mediated foam cell formation in atherogenesis. Science. 2004;306:1558-1561.

17. Malinski T, Taha Z. “Nitric oxide release from a single cell measured *in situ* by a porphyrinic-based microsensor”, Nature, 1992; 358: 676-8.
18. Mason RP, Kalinowshki L, Jacob RF, Jacoby AM, Malinski T, Nebivolol reduces nitroxidative stress and restores nitric oxide bioavailability in endothelium of African Americans. Circulation. 2005, 112:3795-3801.
19. Tuncman G, Hirosumi J, Solinas G, Chang L, Karin M, Hotamisligil G. Functional in vivo interactions between JNK1 and JNK2 isoforms in obesity and insulin resistance. PNAS 2006;103:10741-10746.
20. Lerman, A., Zeiher, A. M. Endothelial Function: Cardiac Events. Circulation 2005; 111:63-8.
21. Osto E, Coppolino G, Volpe M, Cosentino F. Restoring the dysfunctional endothelium. Curr Pharm Des. 2007;13:1053-68.
22. White CR, Darley-Usmar V, Berrington WR, McAdams M, Gore JZ, Thompson JA, Parks DA, Tarpey MM, Freeman BA. Circulating plasma xanthine oxidase contributes to vascular dysfunction in hypercholesterolemic rabbits. Proc Natl Acad Sci USA 1996; 93:8745-9.
23. Ohara Y, Peterson TE, Harrison DG. Hypercholesterolemia increases endothelial superoxide anion production. J Clin Invest 1993; 91:2546-51.
24. Stroes E, Kastelein J, Cosentino F, Erkelens W, Wever R, Koomans H, Luscher T, Rabelink T. Tetrahydrobiopterin restores endothelial function in hypercholesterolemia. J Clin Invest 1997; 99:41-6.
25. Ma XL, Lopez BL, Liu GL, Christopher TA, Gao F, Guo YP, Feuerstein GZ, Ruffolo RRJr, Barone FC, Yue TL. Hypercholesterolemia impairs a detoxification mechanism against peroxynitrite and renders the vascular tissue more susceptible to oxidative injury. Circ Res1997; 80:894-901.

26. Beckam JS, Koppenol WH. Nitric oxide, superoxide and peroxynitrite:the good, the bad and the ugly. Am J Physiol 1996; 271:C1424-37.
27. Zou MH, Leist M, Ullrich V. Selective nitration of prostacyclin synthase and defective vasorelaxation in atherosclerotic bovine coronary arteries. Am J Pathol. 1999;154:1359 –1365.
28. van der Loo B, Labugger R, Skepper JN, Bachschmid M, Kilo J, Powell JM, Palacios-Callender M, Erusalimsky JD, Quaschning T, Malinski T, Gygi D, Ulrich V, Luascher TF. Enhanced peroxynitrite formation is associated with vascular aging. *J Exp Med*. 2000;192:1731–1744.
29. Cosentino F, Eto M, De Paolis P, van der Loo B, Bachschmid M, Ullrich V, Kouroedov A, Delli Gatti C, Joch H, Volpe M, Lüscher TF. High glucose causes upregulation of cyclooxygenase-2 and alters prostanoid profile in human endothelial cells: role of protein kinase C and reactive oxygen species. Circulation. 2003 25;107:1017-23.
30. Camici GG, Schiavoni M, Francia P, Bachschmid M, Martin-Padura I, Hersberger M, Tanner FC, Pelicci P, Volpe M, Anversa P, Lüscher TF, Cosentino F. Genetic deletion of p66(Shc) adaptor protein prevents hyperglycemia-induced endothelial dysfunction and oxidative stress. Proc Natl Acad Sci U S A. 2007;104:5217-22.
31. Kurosawa T, Itoh F, Nozaki A, Nakano Y, Katsuda S, Osakabe N, Tsubone H, Kondo K, Itakura H. Suppressive effects of cacao liquor polyphenols (CLP) on LDL oxidation and the development of atherosclerosis in Kurosawa and Kusanagi-hypercholesterolemic rabbits. Atherosclerosis 2005; 179:237–246.
32. Jessup W.Oxidized lipoproteins and nitric oxide. *Curr Opin Lipidol*. 1996; 7:274 – 280.
33. Oemar BS, Tschudi MR, Godoy N, Brovkovich V, Malinski T, Luscher TF. Circulation. 1998;97:2494-2498.

34. Metzler B, Hu Y, Dietrich H, Xu Q. Increased expression and activation of stress-activated protein kinases/c-Jun NH(2)-terminal protein kinases in atherosclerotic lesions coincide with p53. Am J Pathol. 2000;156:1875-86.
35. Milano G, Morel S, Bonny C, Samaja M, von Segesser LK, Nicod P, Vassalli G. A peptide inhibitor of c-Jun NH2-terminal kinase reduces myocardial ischemia-reperfusion injury and infarct size in vivo. Am J Physiol Heart Circ Physiol. 2007;292:H1828-35.
36. Yoshimura K, Aoki H, Ikeda Y, Fujii K, Akiyama N, Furutani A, Hoshii Y, Tanaka N, Ricci R, Ishihara T, Esato K, Hamano K, Matsuzaki M. Regression of abdominal aortic aneurysm by inhibition of c-Jun N-terminal kinase. Nat Med. 2005;11:1330-8.
37. Yoshimura K, Aoki H, Ikeda Y, Furutani A, Hamano K, Matsuzaki M. Identification of c-Jun N-terminal kinase as a therapeutic target for abdominal aortic aneurysm. Ann N Y Acad Sci. 2006;1085:403-6.
38. Rahaman SO, Lennon DJ, Febbraio M, Podrez EA, Hazen SL, Silverstein RL. A CD36-dependent signaling cascade is necessari for macrophage foam cell formation Cell Met 2006;4211-21.
39. Jaeschke A, Rincon M, Doran B, Reilly J, Neuberg D, Greiner DL, Shultz LD, Rossini AA, Flavell RA, Davis RJ. Disruption of the Jnk2 (Mapk9) gene reduces destructive insulitis and diabetes in a mouse model of type I diabetes. PNAS 2005;102:6931-6935.
40. Borsello T, Clarke PG, Hirt L, Vercelli A, Repici M, Schorderet DF, Bogousslavsky J, Bonny C. A peptide inhibitor of c-Jun N-terminal kinase protects against excitotoxicity and cerebral ischemia. Nat Med. 2003;9:1180-6.
41. Hirosumi J, Tuncman G, Chang L, Görgün CZ, Uysal KT, Maeda K, Karin M, Hotamisligil GS. A central role for JNK in obesity and insulin resistance. Nature. 2002;420:333-6.

Figure Legends

Figure 1. Representative Western blots show phosphorylated JNK (p-JNK) protein expression in aortic lysates from wild-type (WT) after 14 weeks of normal (ND) or high cholesterol diet (HCD). Expression of total JNK was used as a loading control.

Figure 2. (A) Hypercholesterolemia-induced changes in endothelium-dependent relaxation of aortae isolated from WT and *JNK2*-deficient (*JNK2*$^{-/-}$) mice after 14 weeks of normal (ND) or high cholesterol diet (HCD). Line graphs show concentration–response curves to acetylcholine (Ach) during submaximal contraction to norepinephrine (10^{-6} mol/L). (B) Effect of polyethylene glycol-superoxide dismutase (PEG-SOD) on the endothelium-dependent relaxation to acetylcholine in all experimental groups. Results are presented as mean±SEM; *n*=4-6 in each group. *p < 0.05 for WT HCD vs. all other groups.

Figure 3. Bar graphs show the concentration of (A) nitric oxide (NO) and (B) superoxide (O_2^-) produced by a single aortic endothelial cell of WT and *JNK2*$^{-/-}$ mice after 14 weeks of normal (ND) or high cholesterol diet (HCD). Peak concentrations were measured after stimulation with acetylcholine (10^{-7} mol/L). Results are presented as mean±SEM; n=4-6 in each group; *p < 0.05 vs. WT ND. (C) Similar results were obtained by fluorescence detection of O_2^- (red dihydroethidium staining) in freshly isolated aortic segments of WT and *JNK2*$^{-/-}$ mice after ND or HCD, respectively.

Figure 4. (A) Bar graphs show peroxynitrite ($ONOO^-$) concentration produced by a single aortic endothelial cell of WT and *JNK2*$^{-/-}$ mice after 14 weeks of normal (ND) or high cholesterol diet (HCD). $ONOO^-$ was measured simultaneously with NO and O_2^- after stimulation with acetycholine (10^{-7} mol/L). (B) In aortae of WT and *JNK2*$^{-/-}$ mice after ND or HCD, immunostaining for nitrotyrosine (red staining) was detected both in the endothelium and in the media. (C) Bar graphs show TBARS levels in aortae of WT and *JNK2*$^{-/-}$ mice after ND or HCD, respectively. Results are presented as mean±SEM; n=4-6 in each group, *p< 0.05 vs WT ND.

Figure 5. Mn-SOD (A) and EC-SOD (B) protein expression from aortae of WT and *JNK2*$^{-/-}$ mice after 14 weeks of normal (ND) or high cholesterol diet (HCD). Representative Western blots and densitometric quantification are shown. Results are presented as mean±SEM of Mn-SOD and EC-SOD/α-Tubulin expression ratio, n=4-6 in each group. *p< 0.05 vs. ND WT, **p<0.05 vs. *JNK2*$^{-/-}$ ND, †p<0.05 vs. diet-matched WT.). (C) In aortae of WT and *JNK2*$^{-/-}$ mice after ND or HCD, immunostaining for MnSOD (red staining) was detected both in the endothelium and in the media.

Figure 6. eNOS protein expression and phosphorylation in aortic lysates from WT and *JNK2*$^{-/-}$ mice after 14 weeks of normal (ND) or high cholesterol diet (HCD). (A) Representative Western blot and densitometric quantifications are shown for eNOS expression. Results are presented as mean±SEM of eNOS/α-Tubulin expression ratio, n=4-6 in each group. *p< 0.05 for *JNK2*$^{-/-}$ HCD vs. all other groups. (B) Western blot of eNOS phosphorylation (pooled samples of n=3 mice in each group) using β−actin as a loading control.

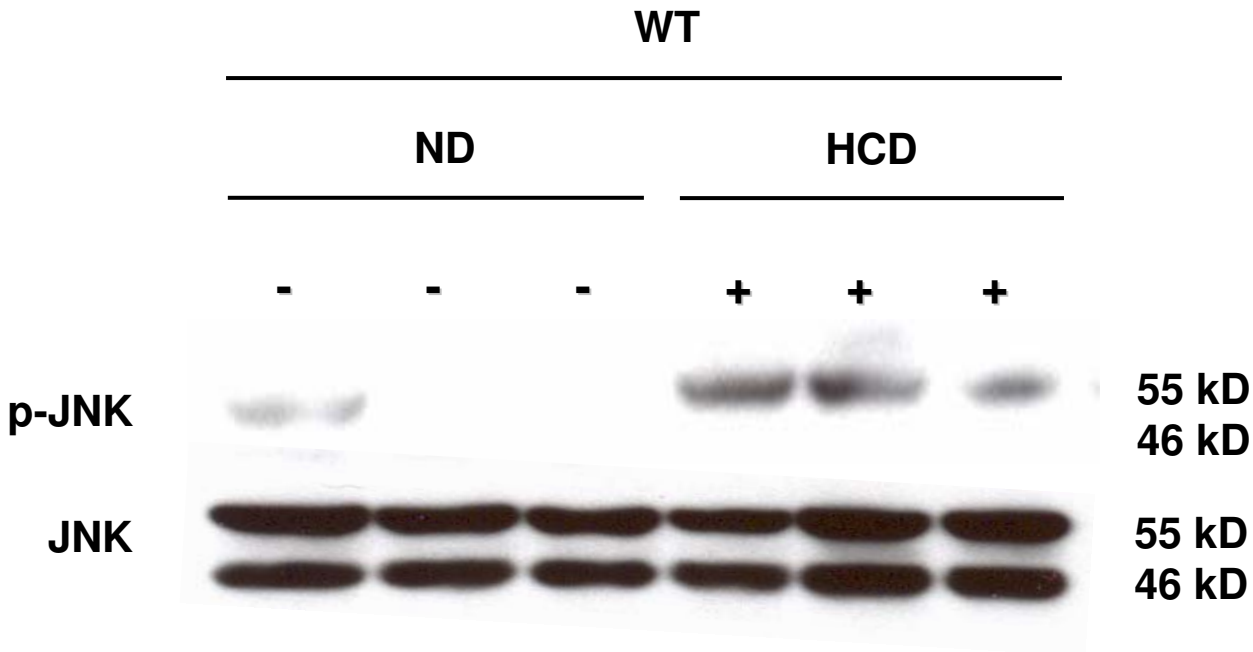

Figure 1

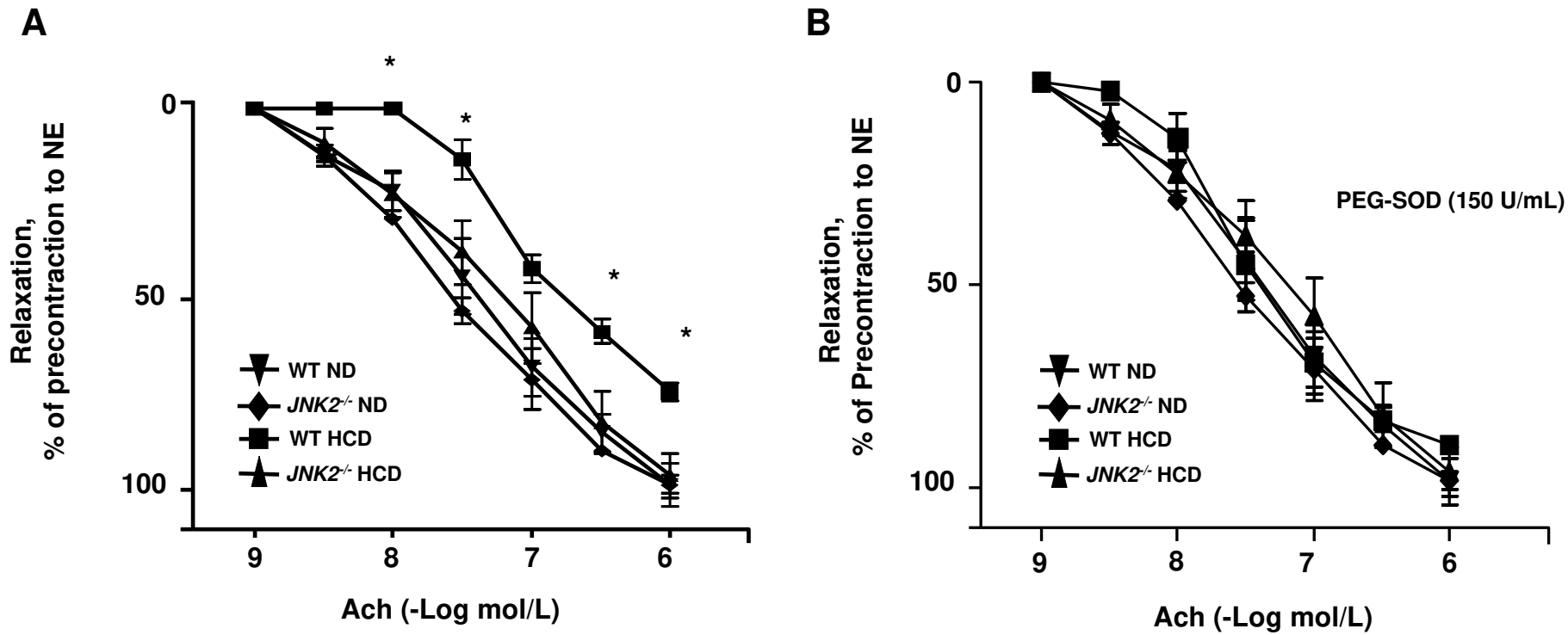
A
B
Relaxation,
% of precontraction to NE
% of Precontraction to NE
0
50
100
9
8
7
6
Ach (-Log mol/L)
WT ND
JNK2-/- ND
WT HCD
JNK2-/- HCD
PEG-SOD (150 U/mL)
*

Figure 2

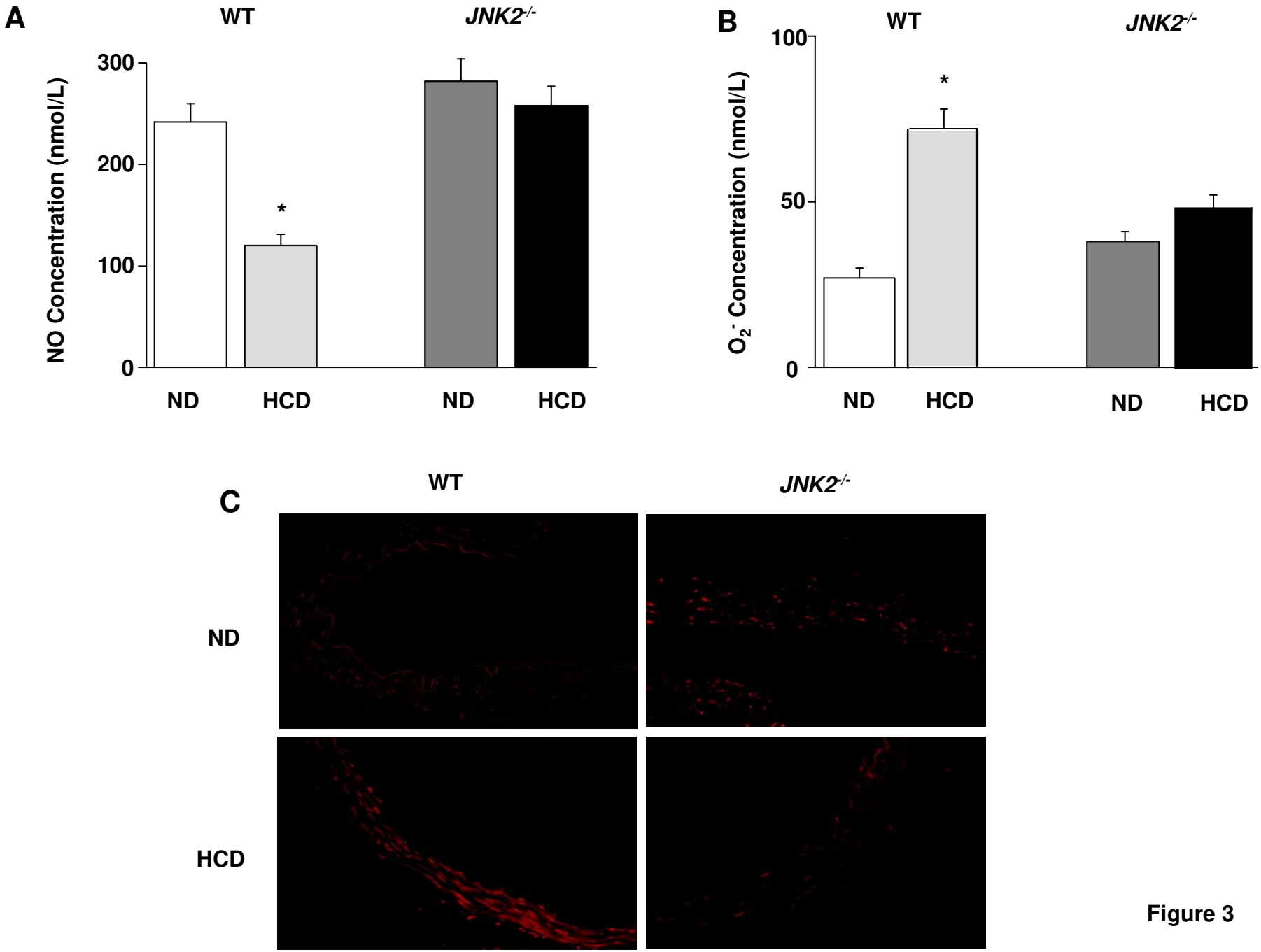
A
WT
JNK2-/-
NO Concentration (nmol/L)
300
200
100
0
*
ND
HCD
ND
HCD
B
WT
JNK2-/-
O2- Concentration (nmol/L)
100
50
0
*
ND
HCD
ND
HCD
C
WT
JNK2-/-
ND
HCD

Figure 3

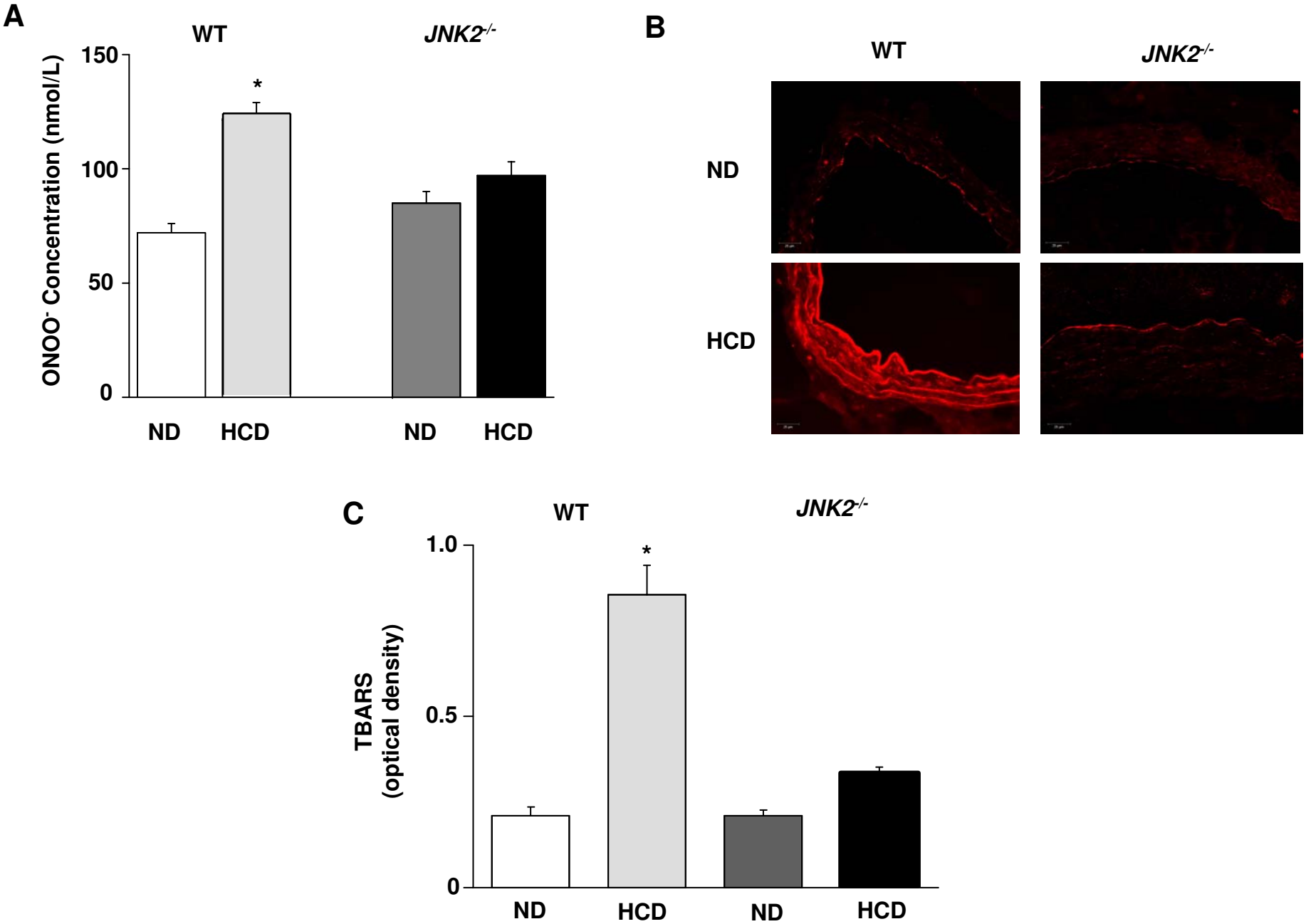
A
WT
JNK2-/-
ONOO- Concentration (nmol/L)
150
100
50
0
*
ND
HCD
ND
HCD
B
WT
JNK2-/-
ND
HCD
C
WT
JNK2-/-
TBARS (optical density)
1.0
0.5
0
*
ND
HCD
ND
HCD

Figure 4

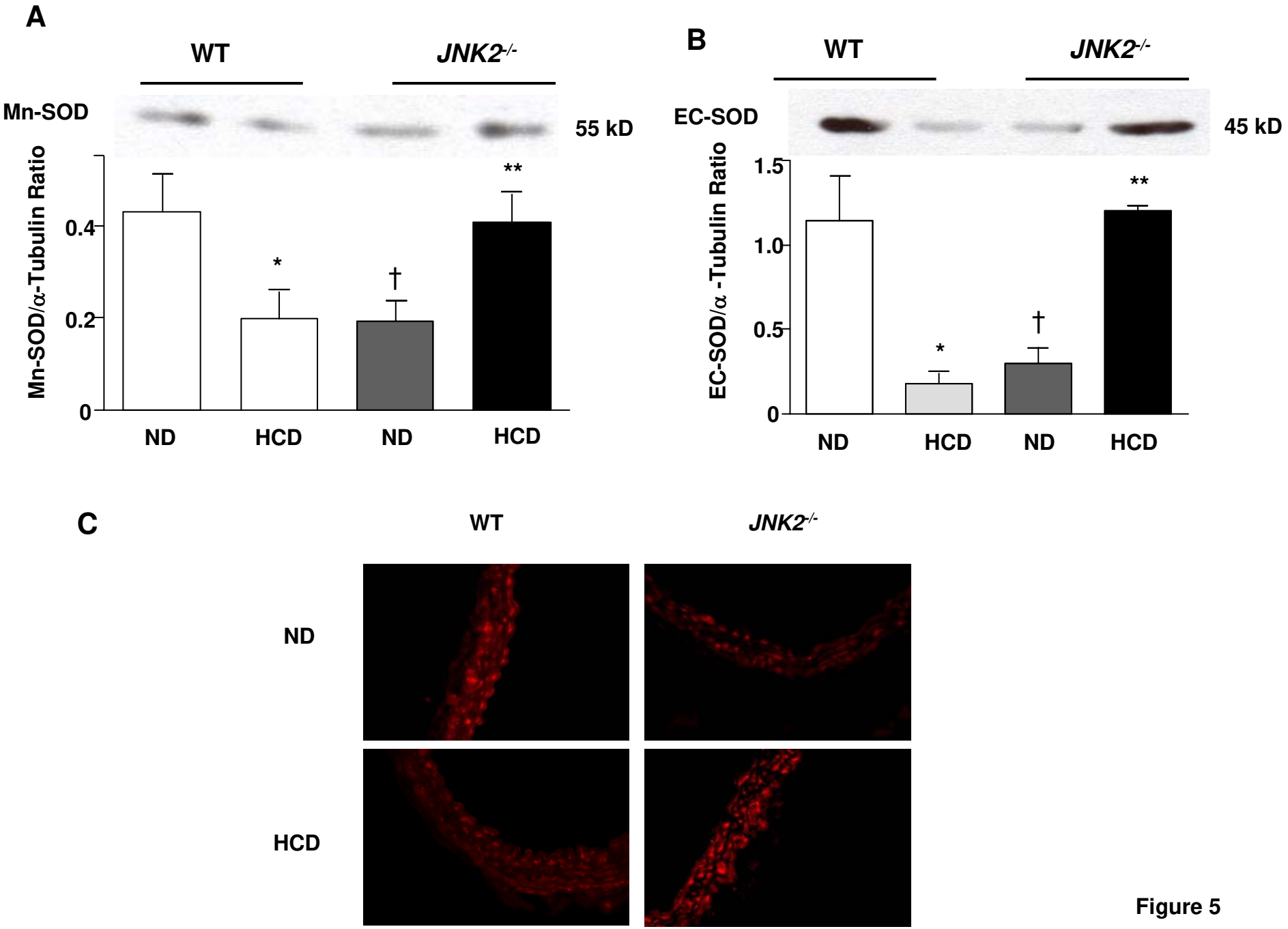
A
WT
JNK2-/-
Mn-SOD
55 kD
Mn-SOD/α-Tubulin Ratio
0.4
0.2
0
*
†
**
ND
HCD
ND
HCD
B
WT
JNK2-/-
EC-SOD
45 kD
EC-SOD/α -Tubulin Ratio
1.5
1.0
0.5
0
*
†
**
ND
HCD
ND
HCD
C
WT
JNK2-/-
ND
HCD

Figure 5

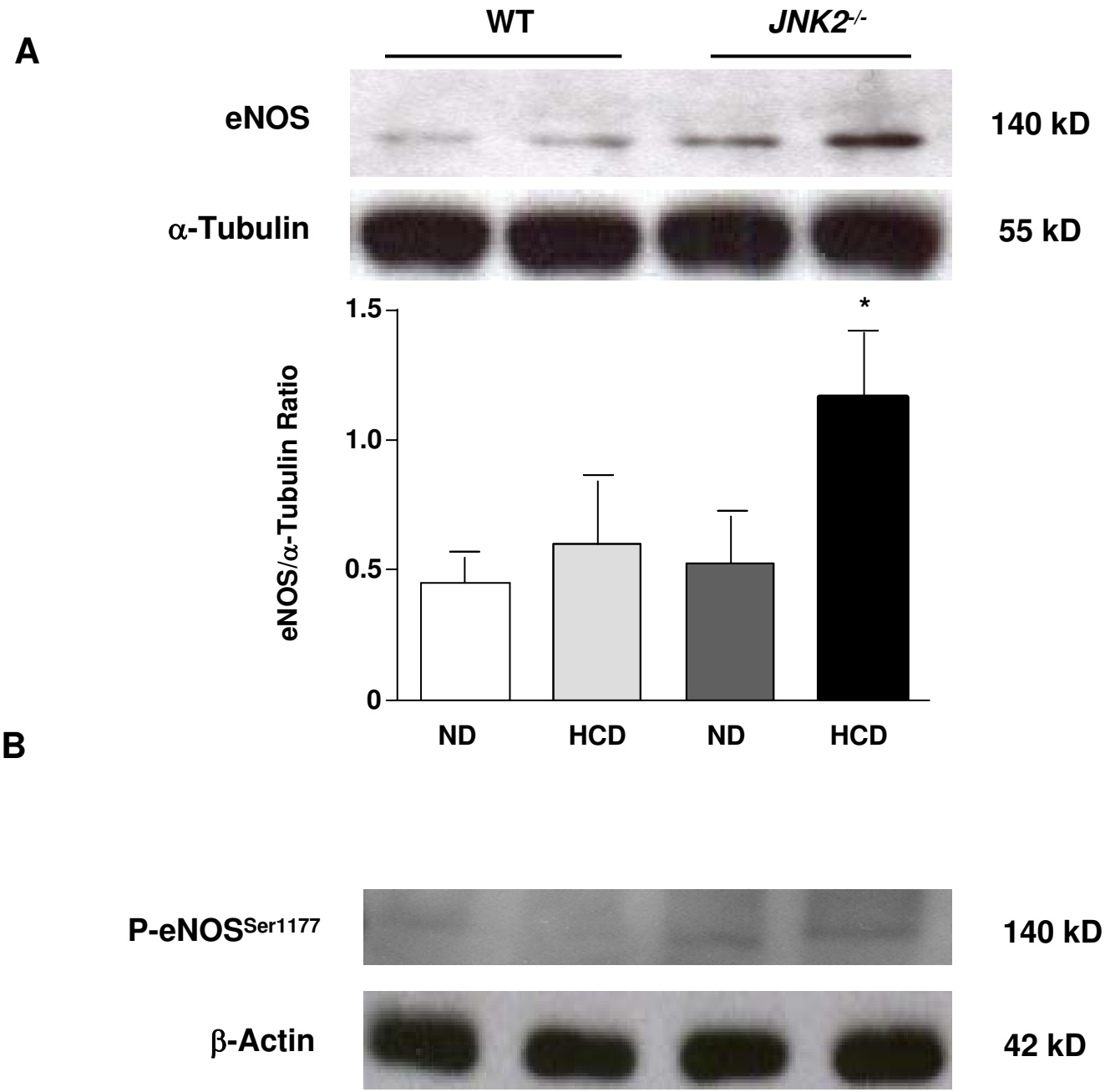
A
WT
JNK2-/-
eNOS
140 kD
α-Tubulin
55 kD
eNOS/α-Tubulin Ratio
1.5
1.0
0.5
0
*
ND
HCD
ND
HCD
B
P-eNOSSer1177
140 kD
β-Actin
42 kD

Figure 6

Table 1. Plasma lipids from *JNK2-/-* and WT littermates after 14 weeks of normal diet (ND) or high cholesterol diet (HCD).

	WD		***JNK2-/-***	
	ND	**HCD**	**ND**	**HCD**
Total cholesterol (mmol/L)	3.3 ± 0.2	7.1 ± 2.4*	3.9 ± 0.3**	9.6 ±1.2*†
Triglycerides (mmol/L)	1.34 ± 0.45	0.79 ± 0.18	1.40 ± 0.6	1.35 ± 0.27
Free fatty acid (mmol/L)	0.54 ± 0.34	0.33 ± 0.07	0.35 ± 0.05	0.34 ± 0.09

Values are mean ± SEM. n=4-6 in each group. *p<0.05 vs ND WT and *JNK2-/-* mice, respectively, *p<0.05 vs diet-matched WT, †p<0.05 vs. HCD WT mice.